Journal of Computational Physics **163,** 313–327 (2000)
doi:10.1006/jcph.2000.6563, available online at http://www.idealibrary.com on IDEAL®

Fractal Behaviour of Diffraction Pattern of Thue–Morse Sequence

Janusz Wolny,* Anna Wnęk,* and Jean-Louis Verger-Gaugry†

*Faculty of Physics and Nuclear Techniques, University of Mining and Metallurgy, al. Mickiewicza 30, 30-059 Krakow, Poland; and †Institut Fourier, UFR de Mathématique, UJF Grenoble, CNRS URA 188, B.P. 74, Domaine Universitaire, 38402 Saint Martin d'Heres, France
E-mail: wolny@novell.ftj.agh.edu.pl

Received February 2, 2000; revised June 9, 2000

The Thue–Morse sequence is an example of an aperiodic structure with a singular continuous contribution to the diffraction pattern. Many satellites observed near the main diffraction peaks have been indexed and their intensities have been numerically calculated. Details of such a calculation are presented for satellite peaks indexed by $1/3$. An average-unit-cell approach was successfully used to describe probabilities of atomic displacements from the points of the reference lattice. For a certain parameterisation of such probabilities, the results of fairly simple integer calculations could be easily generalised. For some defined sets of points, the analytical expressions for diffraction intensities were found and tested numerically on a wide range of scattering vectors and for up to 2^{32} atoms.

Key Words: Thue–Morse sequence; singular continuous diffraction pattern; aperiodic structures; average unit cell; structure factor; Fourier transform; automata sequences; combinatorics on words; structure of quasicrystals; fractals.

INTRODUCTION

The one-sided Thue–Morse sequence can be defined on a two-letter alphabet $\{0, 1\}$, using the following substitution rule $\sigma : \sigma(0) = 0\ 1, \sigma(1) = 1\ 0$ [1–11]. Starting with 0, one obtains the sequence $0110100110010110\ldots$, which is neither periodic nor quasiperiodic. For such a sequence the two figures are replaced by the corresponding two bonds (a and b). In this paper it is assumed that $b = 0.1$ and $a = 10b = 1$ and the "atoms" are placed at the bond's edges (see also [3, 4, 11–13]). In the diffraction pattern of such a structure one can find two components that scale differently with the number of atoms (N). The first component is known as the atomic contribution (Bragg peaks); it has intensities that scale as N^2. The second one is a singular continuous component, which scales fractally with the number of atoms. For the Thue–Morse sequence the numbers of the two bonds

0021-9991/00 $35.00

are equal, and a periodic subset made of every second position, with a periodicity constant equal to $\lambda_0 = (a + b) = 1.1$, can be selected. The corresponding wave vector is then equal to $k_0 = 2\pi/(a + b) \approx 5.71$. Therefore, for the Thue–Morse sequence, there is an average periodic structure with some appropriate decoration of the unit cell. Occupation probabilities of atomic positions in such a unit cell are given by [14–16] $P(0) = 0.5$ and $P(\pm 0.1) = 0.25$, which leads to the following expression for the intensities of Bragg peaks at $k = n \cdot k_0$:

$$\frac{I(k)}{N^2} = \frac{1}{4}[1 + \cos(kb)]^2. \tag{1}$$

Equation (1) gives correct intensities at periodic positions of Bragg peaks and, in general, describes the so-called envelope function shown as a dashed line in Fig. 1a. In the diffraction pattern of the Thue–Morse sequence there is a lot of diffuse scattering, namely the previously mentioned singular continuous part of the diffraction pattern (see Fig. 1b) [17, 18]. It is already known that there is a cumulation of diffuse scattering around $q_0 = k_0/3$, which leads to well-defined satellite reflections around such particular positions of scattering vectors. However, one should remember that peak positions fluctuate around q_0. This feature is also discussed in our paper. As already shown in [14], intensities at satellite positions scale fractally, disappearing gradually from the diffraction pattern with an increasing number of atoms. In the following we describe intensity at satellite positions given by q_0, using the average-unit-cell approach recently developed by Wolny [14, 19–21]. This allows us not only to calculate the fractal exponents for the scaling behavior of diffraction intensities with respect to the number of atoms, but also to write an analytical expression for diffraction intensities obtained for particular numbers of atoms.

AVERAGE-UNIT-CELL APPROACH

Using the concept of reference lattice [14, 20], we can write the structure factor for monoatomic structure as

$$F(k) = Nf \int_{-\lambda/2}^{\lambda/2} P_k(u) \exp(iku)\, du, \tag{2}$$

where $P_k(u)$ is the probability distribution of atomic displacements from the points of the reference lattice. This distribution depends on the scattering vector $k = 2\pi/\lambda$; and for all higher harmonics (i.e., $m \cdot k$, where $m \in \mathbf{Z}$) we have

$$P_{mk}(u) = \sum_{n \in Z} P_k\left(u + n\frac{\lambda}{m}\right) \tag{3}$$

and

$$F(mk) = Nf \int_{-\lambda'/2}^{+\lambda'/2} P_{mk}(u') \cdot e^{imku'} \cdot du' = Nf \int_{-\lambda/2}^{+\lambda/2} P_k(u) \cdot e^{imku} \cdot du. \tag{4}$$

This means that the probability distribution $P_k(u)$, $|u| \le \lambda/2$, describes an average unit cell for the scattering vector k and all its higher harmonics.

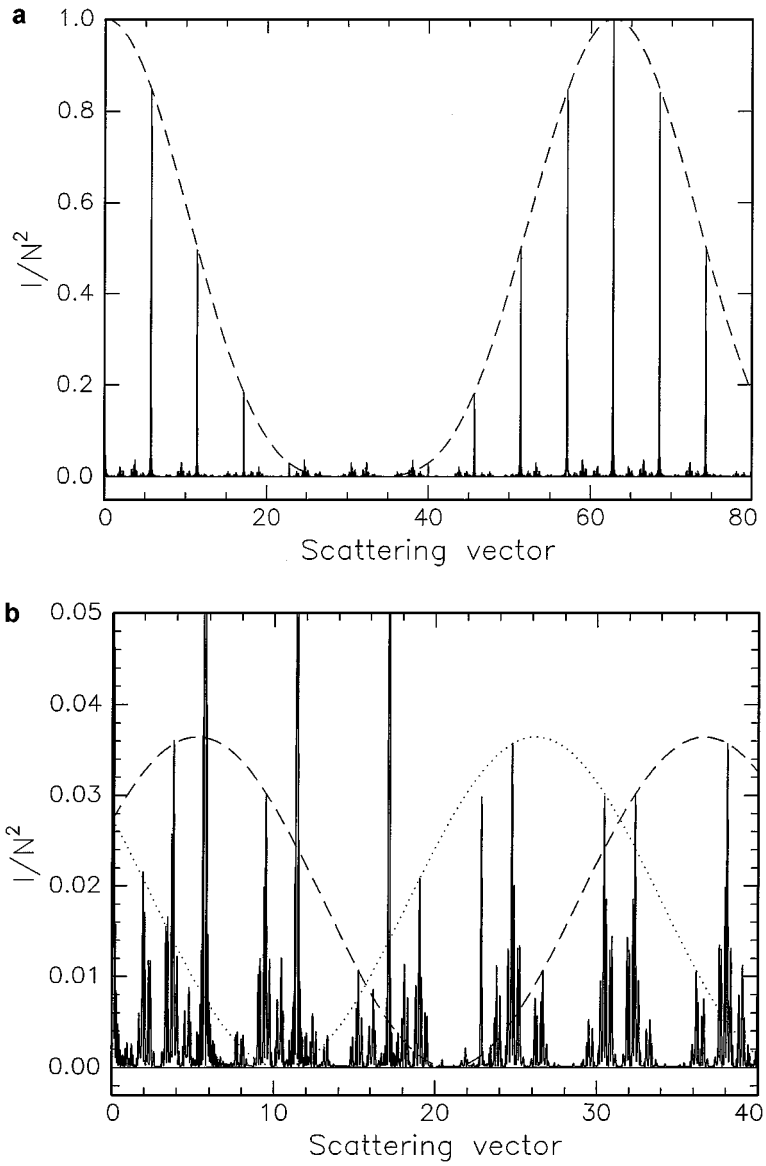

FIG. 1. Diffraction pattern of Thue–Morse sequence. (a) Envelope function given by (1) connects all maxima of the main diffraction peaks. (b) Intensities of satellite reflections are well described by envelope functions given by (10). Envelope curves have been calculated as a function of k for two different satellite positions: $q = +k_0/3$ (dotted line) and $q = -k_0/3$ (dashed line).

It has already been shown in [19] that for a modulated structure the expression for the structure factor of the mth satellite of any nth main reflection is

$$F(nk, mq) = Nf \int_{-u_1}^{u_1} \int_{-v_1}^{v_1} P_{k,q}(u, v) \exp[i(nku + mqv)]\, du\, dv, \tag{5}$$

for $m, n \in \mathbf{Z}$, $u_1 = \pi/k$, $v_1 = \pi/q$, while the probability distribution $P_{k,q}(u, v)$ describes an average unit cell for a series of main reflections and their satellites.

THUE–MORSE SEQUENCE

For the considered Thue–Morse sequence there is a periodic superstructure consisting of every second atom at the lattice positions $x_n = n(a+b), n \in \mathbf{Z}$. The unit cell of this superstructure is decorated by two atoms, one located at position 0 and the other occupying aperiodically the two possible positions at distances a or b from the previous one. For an infinite cluster, occupation probabilities are equal ($P_a = P_b = 1/4$), which leads to the expression for the Bragg reflections given by (1). For any finite structure the difference of these two probabilities is bounded,

$$|P_a - P_b| \leq \frac{1}{N}, \tag{6}$$

where N is the number of atoms in the structure; the proof can be found in [15].

Satellite Reflections at $q = k_0/3$

Using two reference lattices, one with periodicity $\lambda_0 = (a+b) = 1.1$ (corresponding to the scattering vector k_0 of the main reflections) and the other with periodicity equal to $3\lambda_0$ (which corresponds to the scattering vector $q = k_0/3$ describing positions of an appropriate satellite), one gets the probability distribution shown in Fig. 2. The probability distribution in such an average unit cell is non-zero for nine positions only; and, for the number of atoms given by $N = 6n, n \in \mathbf{Z}_+$, the distribution values are related as follows:

$$P_1 = P_4 = P_7 = 1/6 \qquad \text{and} \qquad P_2 + P_3 = P_5 + P_6 = P_8 + P_9 = 1/6. \tag{7}$$

This relation is a consequence of the fact that for each period λ_0 there is an extra atom placed at distance a or b from the super-lattice position (see Table I).

Using (7) and Fig. 2b, a set of three parameters Δ_i ($i = 1, 2, 3$) can be defined, such that

$$\Delta_1 = (P_2 - P_3)N, \qquad \Delta_2 = (P_6 - P_5)N, \qquad \Delta_3 = (P_9 - P_8)N \tag{8}$$

TABLE I
Occupation Probabilities of Nine Different Atomic Positions in 3(a + b) Supercell

n	Position in a $3(a+b)$ supercell	P_n
1	0	1/6
2	b	$P_2 + P_3 = 1/6$
3	a	
4	$a+b$	1/6
5	$(a+b)+b$	$P_5 + P_6 = 1/6$
6	$(a+b)+a$	
7	$2(a+b)$	1/6
8	$2(a+b)+b$	$P_8 + P_9 = 1/6$
9	$2(a+b)+a$	

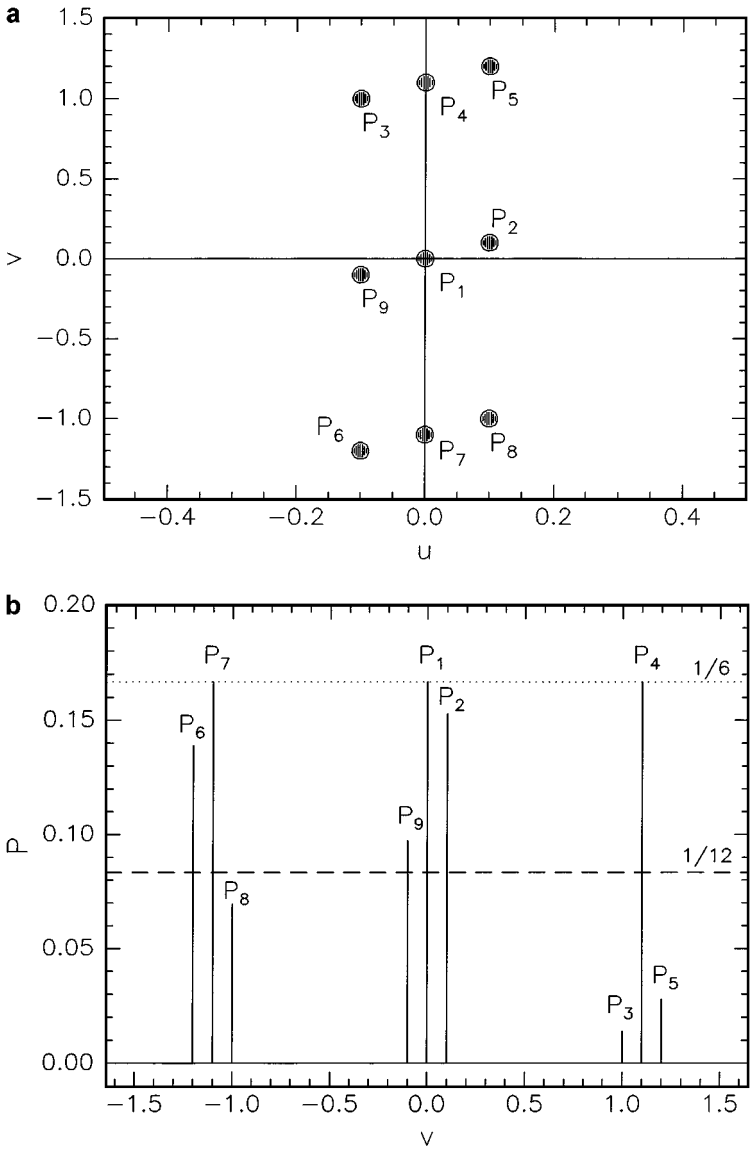

FIG. 2. (a) Positions of non-zero probability distributions of atomic displacements are marked in two-parameter space (u, v). (b) Probability distribution versus v for the number of atoms equal to 72. Peaks marked as P_1, P_4, and P_7 are equal to $1/6$ and correspond to periodical positions of the superstructure. Other probabilities scale with the number of atoms and approach $1/12$ for infinite cluster.

and

$$
\begin{aligned}
P_2 &= \frac{1}{12} + \frac{\Delta_1}{2N}, \qquad & P_3 &= \frac{1}{12} - \frac{\Delta_1}{2N} \\
P_5 &= \frac{1}{12} - \frac{\Delta_2}{2N}, \qquad & P_6 &= \frac{1}{12} + \frac{\Delta_2}{2N} \\
P_8 &= \frac{1}{12} - \frac{\Delta_3}{2N}, \qquad & P_9 &= \frac{1}{12} + \frac{\Delta_3}{2N}.
\end{aligned}
\tag{9}
$$

The structure factor (i.e., the Fourier transform of (9)) is then given by

$$F(k+q) = F_1(k+q) + F_2(k+q), \tag{10}$$

where

$$\begin{aligned} F_1(k+q) &= \frac{N}{6}[1 + 2\cos(q(a+b)) + \cos((k+q)b) + \cos(kb - qa) \\ &\quad + \cos(kb + q(a+2b))] \\ F_2(k+q) &= \frac{\Delta_1}{2}[\exp(i(k+q)b) - \exp(i(qa - kb))] \\ &\quad - i\Delta_2 \sin(kb + q(a+2b)) \\ &\quad - \frac{\Delta_3}{2}[\exp(i(kb - qa)) - \exp(-i(k+q)b)]. \end{aligned} \tag{11}$$

These equations describe correctly the structure factor for each scattering vector given by

$$k_{n,m} = nk_0 + mq_0 \qquad n, m \in \mathbf{Z}; \quad k_0 = \frac{2\pi}{a+b}; \quad q_0 = \frac{k_0}{3}, \tag{12}$$

where nk_0 is the position of the main Bragg peak and mq_0 corresponds to the position of the appropriate mth satellite. The first part of the structure factor (F_1) does not depend on the number of atoms; for $q = 0$, it leads to expression (1) for the diffraction intensity of Bragg reflections.

Parameters Δ_i (shown in Fig. 3) depend on the number of atoms. Figure 3 indicates, and it has also been checked numerically, that for special values assumed by the number of

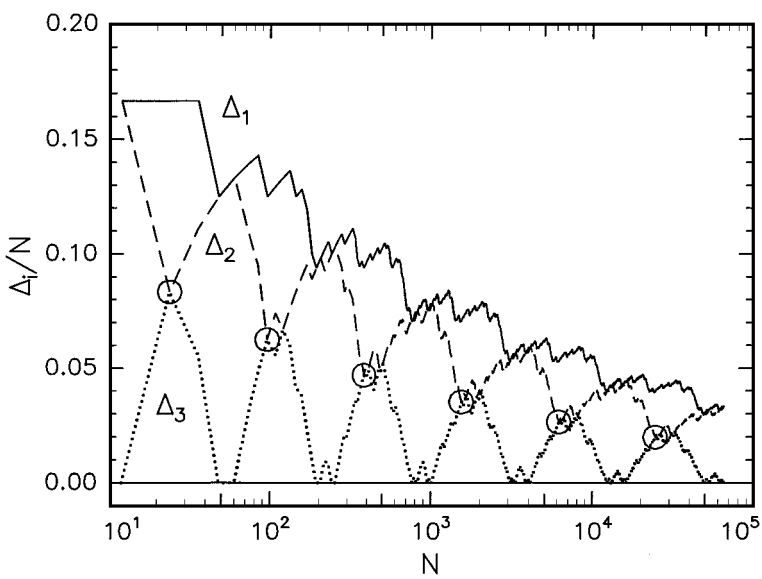

FIG. 3. Plots of Δ_i/N, $i = 1, 2, 3$ versus log N. Open circles mark points for which $N = 6 \cdot 4^n$ and $\Delta_2 = \Delta_3 = \Delta_1/2$.

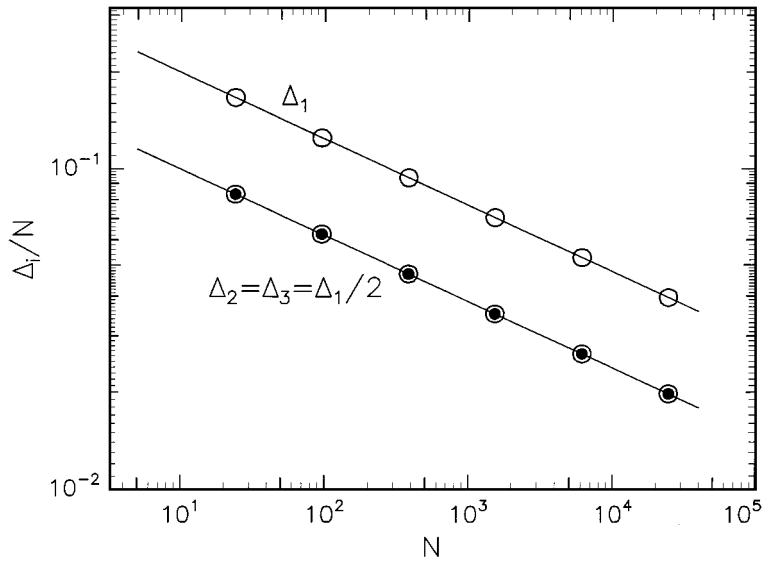

FIG. 4. Double logarithmic plots of Δs divided by N versus the number of atoms, for points marked in Fig. 3. Solid lines represent Eq. (15) with the exponent equal to $\alpha = \log_4 3$.

atoms or more precisely when N is equal to $6 \cdot 4^n$ $(n = 1, 2, \ldots)$, the following relation is fulfilled:

$$\Delta_3 = \Delta_2 = \frac{\Delta_1}{2}. \tag{13}$$

In a double logarithmic scale the Δ plots versus the number of atoms are linear (Fig. 4), with the linear coefficient equal to $\alpha = \log_4(3) \approx 0.7925$. The exact value of the coefficient has been obtained for numerical integer calculations performed for a number of atoms equal to $6 \cdot 4^1 = 24$ and $6 \cdot 4^2 = 96$. For those numbers, Δ_1 is equal to 4 or 12, which corresponds to probabilities $P_2 = 4/24$ or $14/96$ and $P_3 = 0$ or $2/96$, respectively. The plots of Δ multiplied by a factor of $N^{-\alpha}$ versus the number of atoms (Fig. 5) are almost constant (within the range of some fluctuations) in the logarithmic scale of N; therefore,

$$\Delta_{\mathrm{i}} \propto N^{\alpha}, \qquad \text{where } \alpha = \log_4(3). \tag{14}$$

More precisely, for $N = 6 \cdot 4^n$ $(n = 1, 2, 3, \ldots)$,

$$\Delta_1 = \frac{2N}{9}\left(\frac{3}{4}\right)^n = \frac{2N}{9}\left(\frac{3}{4}\right)^{\log_4(N/6)} = \frac{4}{3}\left(\frac{N}{6}\right)^{\alpha} \tag{15}$$

and

$$\Delta_3 = \Delta_2 = \Delta_1/2.$$

These relations have been checked in our "computer experiment."

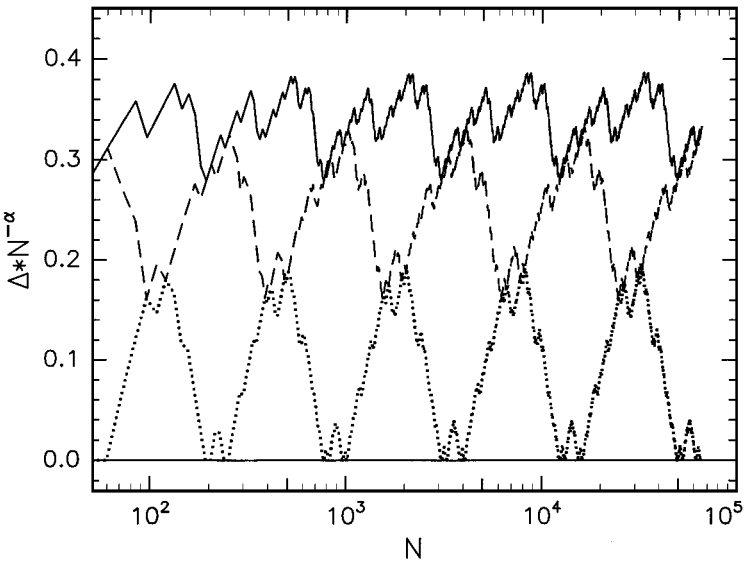

FIG. 5. Parameters Δ_i $(i = 1, 2)$ multiplied by a factor of $N^{-\alpha}$ versus logarithm of the number of atoms. Periodic plots with periodicity constant equal to log 4 can be found.

Number of Points Equal to $N = (2m) \cdot 6$, $m \in \mathbf{Z}$

It has been checked numerically that for each $N = (2m) \cdot 6$, $m \in \mathbf{Z}_+$ (i.e., for all even multiples of 6),

$$\Delta_1 - \Delta_2 - \Delta_3 = 0 \tag{16}$$

and $\Delta_i \cdot N^{-\alpha}$ (i.e., the Δ product with the number of atoms to the power of $-\alpha$) is a periodic function of $\log N$, with a periodicity constant equal to log 4. This allows us to plot $\Delta_i \cdot N^{-\alpha}$ versus ξ, where

$$\xi \equiv \log_4 N \mod 1, \tag{17}$$

which is shown in Fig. 6a. For each delta, a common curve is obtained, which is independent of the number of atoms. Actually, the curves look rather complicated, and a more general expression cannot be given yet. However, we have found the exact values for some special points. The two sets of points are as follows:

Set I:

$$\begin{aligned} N &= 24 \sum_{m \in \mathbf{Z}_+} \beta_m \cdot 4^m, \qquad \text{where } \beta_m \in \{0, 1\}, \\ \Delta_1 &= 4 \sum_{m \in \mathbf{Z}_+} \beta_m \cdot 3^m, \qquad \Delta_3 = \Delta_2 = \frac{\Delta_1}{2}. \end{aligned} \tag{18}$$

Some examples of such numbers are

$$(N, \Delta_1) \in \{(24, 4), (96, 12), (120, 16), (384, 36) \ldots\}.$$

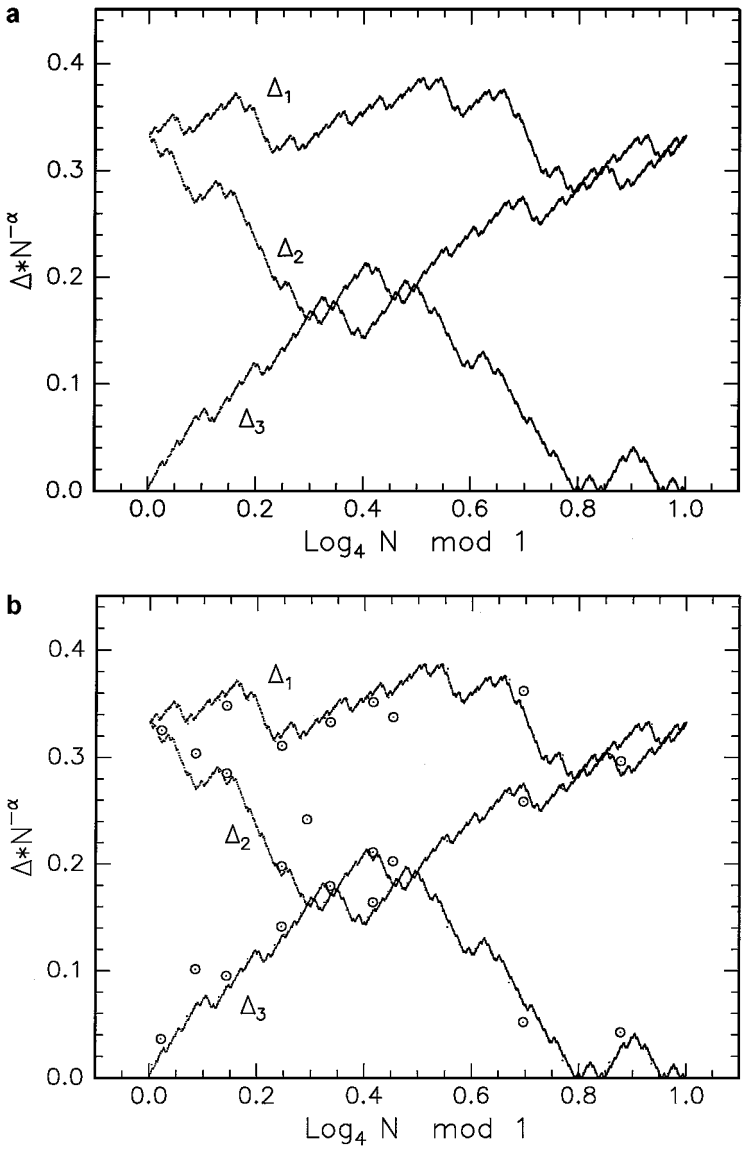

FIG. 6. Plots of $\Delta_i \cdot N^{-\alpha}$ $(i = 1, 2, 3)$ versus $\xi = [\log_4 N \bmod 1]$ for the number of atoms equal to even (a) and odd (b) multiples of 6. The first ten odd multiples are marked as open circles.

Set II:

$$N = 12 \sum_{m \in \mathbf{Z}_+} \beta_m \cdot 4^m, \qquad \text{where } \beta_m \in \{0, 1\},$$
$$\Delta_1 = 2 \sum_{m \in \mathbf{Z}_+} \beta_m \cdot 3^m, \qquad \Delta_2 = \Delta_1, \qquad \Delta_3 = 0. \tag{19}$$

Some examples of such numbers are

$$(N, \Delta_1) \in \{(12, 2), (48, 6), (60, 8), (192, 18) \ldots\}.$$

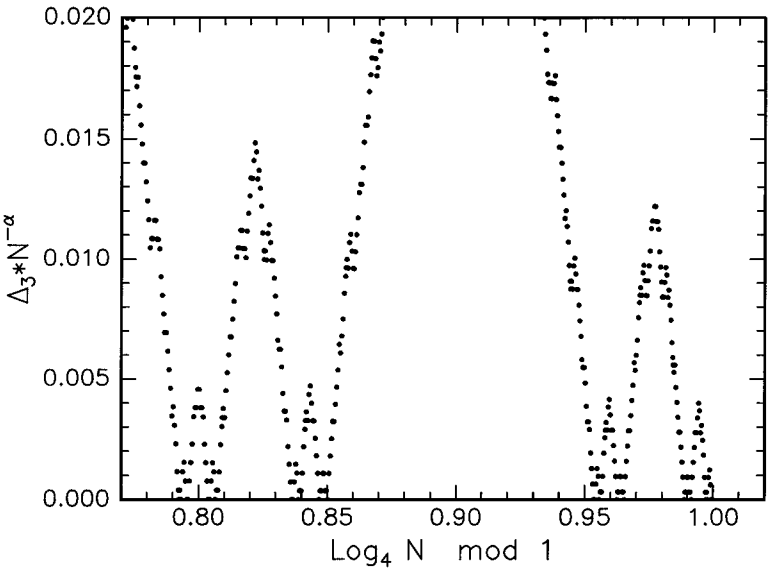

FIG. 7. Plot of $\Delta_3 \cdot N^{-\alpha}$. Δ_3 equals to zero for $N = 12\sum_{m\in\mathbf{Z}_+}\beta_m \cdot 4^m$; where $\beta_m \in \{0, 1\}$.

Those two sets give an infinite number of different points in Fig. 6a. More details for Set II can be found in Fig. 7. Those points can be easily ordered in a sequence as follows:

$$\text{Series 1:}\quad \xi = \left\{\log_4\left[3\left(1+\frac{1}{4}\right)\right], \log_4\left[3\left(1+\frac{1}{4}+\frac{1}{4^2}\right)\right], \ldots\right\}$$
$$= \{0.953, 0.989, \ldots, 1\};$$
$$\text{Series 2:}\quad \xi = \left\{\log_4\left[3\left(1+\frac{1}{4^2}\right)\right], \log_4\left[3\left(1+\frac{1}{4^2}+\frac{1}{4^3}\right)\right], \ldots\right\}$$
$$\approx \{0.836, 0.847, \ldots, 0.850\};$$
$$\text{Series 3:}\quad \xi = \left\{\log_4\left[3\left(1+\frac{1}{4^3}\right)\right], \log_4\left[3\left(1+\frac{1}{4^3}+\frac{1}{4^4}\right)\right], \ldots\right\}$$
$$\approx \{0.796, 0.806, \ldots, 0.807\};$$
$$\vdots$$
$$\text{Series } i\text{:}\quad \xi = \left\{\log_4\left[3\left(1+\frac{1}{4^i}\right)\right], \log_4\left[3\left(1+\frac{1}{4^i}+\frac{1}{4^{i+1}}\right)\right], \ldots\right\};$$
$$\vdots$$

and so on.

Number of Points Equal to $N = (2m+1)\cdot 6$, $m \in \boldsymbol{Z}$

For all numbers of atoms equal to odd multiples of 6, the positions of points for each Δ_i (Fig. 6b) depart from the common curves shown in Fig. 6a for even multiples. However,

such differences decrease rapidly to zero as N^{-1}. The first 10 points in this figure are marked with open circles. For N above 100 one can hardly see any difference from the previous behaviour, with the points almost lined up along the common curve. One can conclude that for a large enough number of atoms (i.e., for more than a few hundred atoms), there are almost no differences between the diffraction pattern obtained for the number of atoms equal to the neighbouring numbers given by even and those given by odd multiples of 6.

DIFFRACTION ANALYSIS

Using formulas (10) and (11), one can calculate intensities of diffraction peaks for the scattering vectors given by (12)

$$I = F_{\text{real}}^2 + F_{\text{imag}}^2, \tag{20}$$

where F_{real} and F_{imag} are the real and imaginary parts of the structure factor, respectively. The formulas can be essentially reduced for certain points described by (18) and (19). The results are as follows:

Set I:

$$\begin{aligned} F_{\text{real}}(q) &= \frac{N}{6}[1 + 2\cos(q(a+b)) + \cos(qb) + \cos(qa) + \cos(q(a+2b))] \\ &\quad + \frac{3}{4}\Delta_1[\cos(qb) - \cos(qa)] \\ F_{\text{imag}}(q) &= \frac{\Delta_1}{4}[\sin(qb) - \sin(qa) - 2\sin(q(a+2b))], \end{aligned} \tag{21}$$

where Δ_1 is given by (18). This is the envelope function plotted in Fig. 8a; it correctly describes intensities at any position of the main peaks and their satellites given by (12).

Set II:

$$\begin{aligned} F_{\text{real}}(q) &= \frac{N}{6}[1 + 2\cos(q(a+b)) + \cos(qb) + \cos(qa) + \cos(q(a+2b))] \\ &\quad + \frac{1}{2}\Delta_1[\cos(qb) - \cos(qa)] \\ F_{\text{imag}}(q) &= \frac{\Delta_1}{2}[\sin(qb) - \sin(qa) - 2\sin(q(a+2b))], \end{aligned} \tag{22}$$

where Δ_1 is given by (19). The appropriate plot of the envelope function is shown in Fig. 8b. The two envelope functions in Figs. 8a and 8b have been calculated using two different formulas ((21) and (22)). There is only a small difference between those envelopes, as they correctly describe the intensities of the main reflections and their satellites. The scaling exponent for the diffraction intensities of satellite reflections is $2\alpha = 2\log_4 3$, which is very close to the one obtained previously [14].

In Figs. 8a and 8b one can see small differences between the envelope function and the maximum intensities of the appropriate satellites because the maximum intensity does not correspond to the exact position of the satellite with index equal to $1/3$. The small shift from

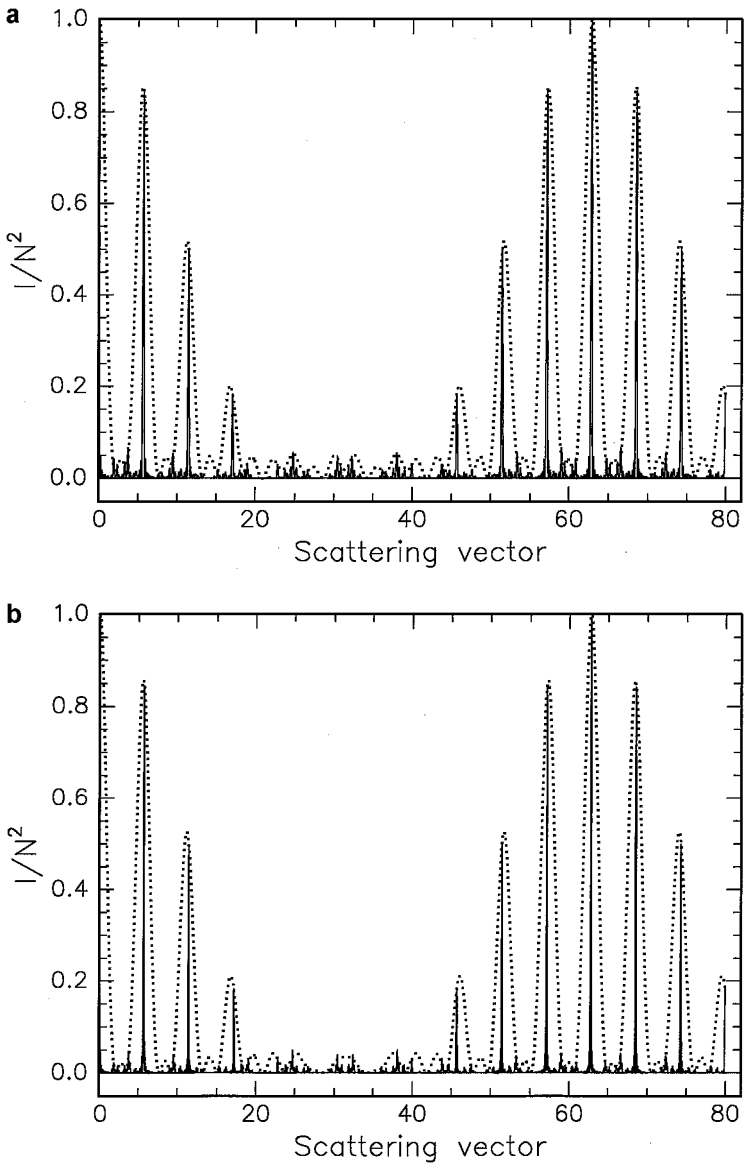

FIG. 8. Diffraction patterns of the Thue–Morse sequence and corresponding envelope functions obtained for different numbers of atoms: (a) $N = 96$ is the second point of Set I (18) and the envelope function was calculated according to (21); (b) $N = 60$ is the third point of Set II (19) and the envelope function was calculated according to (22); (c) $N = 144$ is the number of atoms for which satellites are placed almost at perfect positions (see Fig. 9); in this case, a general expression (11) has been used for the envelope function calculation.

such a particular position is shown in Fig. 9. It oscillates and goes to zero for the number of atoms increasing to infinity. However, it should be stressed that for any scattering vector given by (12), the envelope function gives exactly the same value as the Fourier transform. A special test has been also performed for $N = 144$, when the shift of peak position is almost zero (Fig. 9). For this particular number, the envelope function fits the intensities of the satellites almost perfectly (Fig. 8c). It should be noted that Figs. 1b and 8c show the same diffraction pattern (i.e., for $N = 144$) but the diffraction peaks are connected by

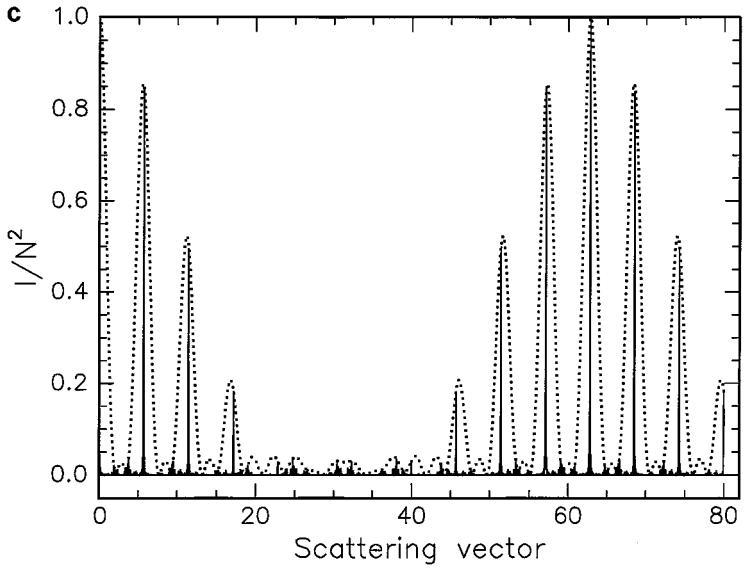

FIG. 8—*Continued*

different envelope functions given by (11). In Fig. 1b, the two different curves are plotted as a function of k (11), for $q = \pm k_0/3$ respectively; and in Fig. 8c the envelope curve is plotted as a function of q (11), for $k = 0$.

For satellites indexed by $1/5$ and $1/7$, similar properties have been observed [21]. Fractal exponents have been determined to be equal to $\alpha = \log_{16} 5$ for index equal to $1/5$ and $\alpha = \log_{64} 7$ for index equal to $1/7$. Properly defined Δ parameters can be expressed similarly to (18) and (19), but the coefficients must be changed. For example, when the satellite index

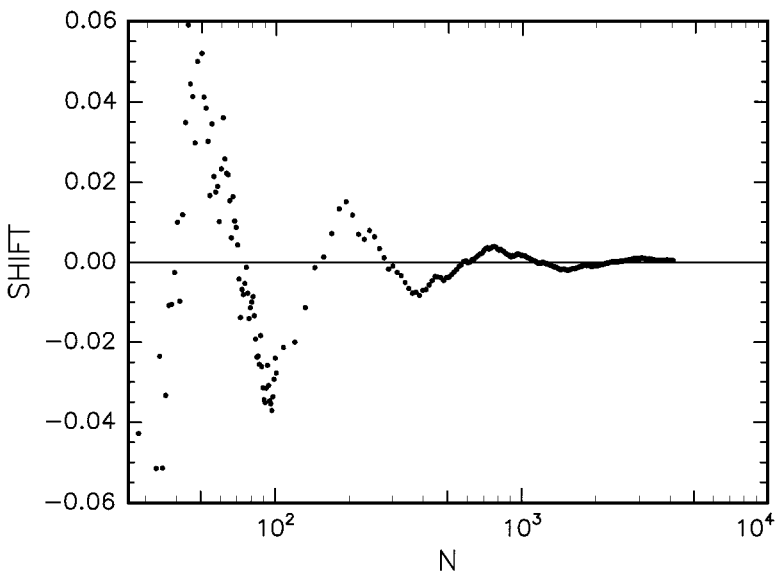

FIG. 9. Shift of peak position with respect to the perfect position of the satellite indexed by $4 + 1/3$, versus the number of atoms in cluster.

is equal to $1/5$, the value of the base of the power expansion for N in (18) and (19) should be changed from 4 to 4^2, and for Δ_1, from 3 to 5.

CONCLUSIONS

In this paper, the average-unit-cell approach has been used for the diffraction analysis of singular continuous diffraction patterns of the Thue–Morse sequence. For satellite reflections with indices equal to $1/3$ of the main Bragg peaks, an average unit cell was constructed in the space defined by two variables, u and v. The probability distribution obtained is nonzero at only nine positions (Fig. 2a), which has allowed us to calculate envelope functions for the main reflections as well as for the satellites. We noticed that probability distributions depend on three parameters Δ_i ($i = 1, 2, 3$) defined by (8). For such Δ's, a general expression for the structure factor has been obtained (11). The Δ parameters depend on the number of atoms, scaling as N^α [$\alpha = \log_4 3$]. For numbers of atoms equal to even multiples of 6, formula (16) holds, and only two Δ's are independent. As a result of our computer experiment, we also found that for some specially defined numbers of atoms (i.e., for Sets I and II), relations (18) and (19) hold respectively, and one Δ parameter is enough to describe intensities of the main reflections and their satellites. It has been shown that for double logarithmic plots, Δ's change periodically with the number of atoms, with the periodicity constant equal to log(4), along a line with a slope equal to some fractal exponent. After appropriate scaling of the Δ's (i.e., multiplication by the factor $N^{-\alpha}$) and after introduction of a new variable ξ (17), a common curve (Fig. 6a) is obtained for all numbers of atoms. A similar curve is also obtained for all odd multiples of 6 as a limit of the number of atoms going to infinity. This saw-like curve is rather complicated and analytical expressions have been suggested for special sets of numbers only (i.e., Set I given by (18) and Set II by (19)). For those particular numbers, exact formulas for diffraction intensities have been written as (21) and (22).

All the formulas in this paper have been tested numerically using integer calculations for the number of atoms limited by 2^{32}. Exact integer calculations and a wide range of N allow us to formulate more general conclusions. However, strict mathematical proofs (in progress) are still required. Some results are already available and will be published separately [15, 16].

Similar results have been obtained for all prime numbers less than or equal to 19, except for 17, where the fractal exponent has been approximated as equal to 0.633 ± 0.0002, which corresponds to the already known value $\alpha = \{\log 17 + 2\log(4 + \sqrt{17})\}/16 \log 2$. More details of calculations will be published elsewhere. The next singular number is expected for $m = 41$. However, the numerical calculations require calculations for integer numbers more than 2^{32} and are in progress.

This paper is an example of a simple "computer experiment." In such an experiment, calculations are performed for integer numbers only, and the strictly valid results can be easily generalised and checked for arbitrarilry large numbers. Any appropriate hypothesis can then be proven for arbitrarily large numbers, and its validity extrapolated for the number of points to infinity. Results of such computer experiments can serve as a substitute for an appropriate mathematical proof.

ACKNOWLEDGMENTS

Discussions with J. P. Gazeau and L. Pytlik were very helpful. Financial support from the Polish Committee for Scientific Research under Grant 2 P03B 041 16 is also acknowledged.

REFERENCES

1. M. Morse, *Trans. Am. Math. Soc.* **22**, 84 (1921).
2. A. Thue, *Norske vid. Selsk. Skr.* I. *Mat. Nat. Kl. Christiania* **7**, 1 (1903); **13**, 1 (1912).
3. J.-P. Allouche and M. Mendes France, Automata and automatic sequences, in *Beyond Quasicrystals*, edited by F. Axel and D. Gratias, Les Editions de Physique (Springer-Verlag, Berlin, 1995), p. 293.
4. M. Queffelec, Dynamical Systems—Spectral Analysis, Lecture Notes in Mathematics (Springer-Verlag, Berlin, 1987), Vol. 1294.
5. M. Queffelec, Spectral study of automatic and substitutive sequences, in *Beyond Quasicrystals*, edited by F. Axel and D. Gratias, Les Editions de Physique (Springer-Verlag, Berlin, 1995), p. 369.
6. J. M. Luck, *Phys. Rev. B* **39**, 5834 (1989).
7. F. Axel, J. P. Allouche, M. Kleman, and M. Mendes France, *J. Phys. (Paris)* **47**, C3 (1986).
8. F. Axel and J. Peyriere, *C. R. Acad. Sci., Ser. 2* **306**, 179 (1988).
9. R. Riklund, M. Severin, and Y. Liu, J., *Mod. Phys. B* **1**, 121 (1987).
10. Z. Cheng, R. Savit, and R. Merlin, *Phys. Rev. B* **37**, 4375 (1988).
11. M. Kolar, B. Iochum, and L. Raymond, *J. Phys. A Math. Gen.* **26**, 7343 (1993).
12. J. M. Luck, C. Godreche, A. Janner, and T. Janssen, *J. Phys A Math. Gen.* **26**, 1951 (1993).
13. F. Gähler and R. Klitzing, The diffraction pattern of self-similar tilings, in *The Mathematics of Long-Range Aperiodic Order*, edited by R.V. Moody, NATO Series (Kluwer Academic, Dordrecht, 1997), p. 141.
14. J. Wolny, The reference lattice concept and its application to the analysis of diffraction patterns, *Philos. Mag. A* **77**, 395 (1998).
15. J.-L. Verger-Gaugry, J. Wolny, Generalized Meyer sets and Thue–Morse quasicrystals with toric internal space, *J. Phys. A* **32**, 6445 (1999).
16. J.-L. Verger-Gaugry, J. Wolny, J. Patera, Mathematical quasicrystals with toric internal spaces, diffraction and Thue–Morse sequence, preprint (1999).
17. M. Keane, Generalized Morse sequence, *Z. Wahrscheinlichkeit* **10**, 335 (1968).
18. J. Peyriere, Ann. Inst. Fourier, Grenoble **25**, 127 (1975).
19. J. Wolny, Average unit cell of the Fibonacci chain, *Acta Crystallozr. Sect. A* **54**, 1014 (1998).
20. J. Wolny, Kwazikrysztaly i inne dwuwymiarowe uklady o zabronionej symetrii, *Zesz. Nauk. Akad. Gorn. Hutn. a Fiz.* **23**, 1 (1991).
21. J. Wolny, A. Wnek, J.-L. Verger-Gaugry, L. Pytlik, Average unit-cell approach to diffraction on Thue-Morse sequence and decorated quasicrystals, in *Proc. 7th Int. Conf. on Quasicrystals*, preprint (1999).